REPORT DOCUMENTATION PAGE

Form Approved
OMB No. 0704-0188

1. AGENCY USE ONLY (*Leave Blank*)	2. REPORT DATE	3. REPORT TYPE AND DATES COVERED
	4/15/95	Scientific & Technical 9/15/94-3/15/95

4. TITLE AND SUBTITLE
Cellular Approaches to The Treatment of Clinical Shock

5. FUNDING NUMBERS
DAAH01-94-C-R295

6. AUTHOR(S)
Guy Miller

7. PERFORMING ORGANIZATION NAME(S) AND ADDRESS(ES)
Galileo Laboratories, INC.
1311 Orleans Drive
Sunnyvale, CA 94089

8. PERFORMING ORGANIZATION REPORT NUMBER

9. SPONSORING/MONITORING AGENCY NAME(S) AND ADDRESS(ES)
Advanced Research Projects Agency
3701 North Fairfax Drive
Arlington, VA 22203-1714
(Dr. Ira Skurnick)

10. SPONSORING/MONITORING AGENCY REPORT NUMBER

11. SUPPLEMENTARY NOTES

12a. DISTRIBUTION/AVAILABILITY STATEMENT
No limitations on availability/distribution

12b. DISTRIBUTION CODE

13. ABSTRACT (*Maximum 200 words*)

A convenient model system has been developed to examine the effects of energy depletion on cells as a model of clinical shock. Cells are grown on microporous polycarbonate transwells and placed into proximity to a pH sensing silicon chip. Cellular proton flux is recorded as a function of time (extracellular acidification rate). Four cell lines were examined for their suitability in this model system: 1) liver cells; 2) kidney cells; 3) intestinal cells; and 4) tumor cells. Changes in proton flux correlated with other standard viability indices. Further work is being performed to characterize more fully this system.

14. SUBJECT TERMS	15. NUMBER OF PAGES
cell metabolism, clinical shock, golden hour, combat injury	12
	16. PRICE CODE

17. SECURITY CLASSIFICATION OF REPORT	18. SECURITY CLASSIFICATION OF THIS PAGE	19. SECURITY CLASSIFICATION OF ABSTRACT	20. LIMITATION OF ABSTRACT
UNCLASSIFIED	UNCLASSIFIED	UNCLASSIFIED	UL

Scientific & Technical Report

April 15, 1995

Sponsored by:

Advanced Research Projects Agency

ARPA Order 5916

Issued by U.S. Army Missile Command Under
Contract No. DAAH01-94-C-R295

Galileo Laboratories, Inc.
1311 Orleans Drive
Sunnyvale, CA 94089
galileo@moldev.com

Guy Miller, MD, PhD
Chairman, CEO
408-747-3594

Effective Date: 9/15/94
Expiration Date: 4/15/95
Reporting Period: 9/15/94-3/15/95

Treatment of Clinical Shock

I. TABLE OF CONTENTS

II. Introduction

II.A. Background

In instances of cardiogenic or hemorrhagic shock, the causative factor leading to injury is a critical loss of oxygen delivery to tissues. In both clinical situations, significant advances have been realized in the design and implementation of strategies to restore oxygen delivery. A partial list of therapies include: cardio-pulmonary resuscitation; transfusion therapy, blood substitutes and intravascular volume expanders; vasopressor pharmacology; and extracorporeal membrane oxygenation, intravenous oxygenation. While, the success of these therapies have been aided by both diagnosis [pulmonary artery catheters, gastric tonometry] and implementation [military: far-forward hospitals/triage; civilian: shock-trauma centers],i.e., the golden hour, physiologic support alone does not fully address the extent of the underlying [cellular] injury.

That the problem of hemorrhagic shock extended beyond replacement of oxygen carrying capacity or delivery was described and elaborated upon by Shires who demonstrated that simple restoration of oxygen carrying capacity in instances of prolonged hypotension was insufficient to restore organ function. The concept of the cellular basis of shock was advanced in the 1960's and 1970's to explain these observations. The cellular basis of shock has now been extended within the last decade to include the constellation of systemic perturbations [inflammatory response, secondary mediators] that result in the manifested shock syndrome.

II.B. Problem

The mainstay for the management of clinical shock is supportive therapy and a correction of the causal factor(s). The principles that guide supportive therapy are based upon promoting oxygen delivery to vital organs systems by an optimization of physiologic function. Through the restoration/maintenance of oxygen delivery by physical and pharmacological means, critical tissue function is maintained affording the chance for the self repair of sub-lethal cellular injury. With a temporization of a sub-lethal cellular injury, recovery is usually afforded. Such a transition to recovery is not witnessed when a critical mass [function] of cells are rendered irreversibly injured. Hence, strategies to address the cellular basis of shock are needed to advance new

Hence, strategies to address the cellular basis of shock are needed to advance new therapies.

IIC. Specific Aims of SBIR

The specific aims of this effort were: 1) the development of a more convenient means to screen naturally occurring, semi-synthetic and synthetic potential therapeutics, against a cellular model of shock; and 2) begin to elucidate the effect of putative cytoprotectants on such isolated cell model systems of shock.

III. Methodology

III.A. Microphysiometry

III.A.i. Principle

Cells are grown in cell culture on a semipermeable membrane and placed into close proximity to a sensitive proton sensor- light addressable potentiometric sensor [LAPS]. Protons are generated through a variety of processes including oxidative phosphorylation and glycolysis. Changes in the rate of proton excretion, i.e., metabolic activity, are recorded per unit time. In this manner, substrate flux, and metabolic rate is assessed using proton flux as a proxy.

III.A.ii. Method(s)

Microphysiometer studies were carried out using the 8 channel Cytosensor® [Molecular Devices Corporation, Sunnyvale, CA]. Cells are seeded on microporous [3 μm pore size] polycarbonate transwells [Molecular Devices Corporation, Sunnyvale, CA] under conditions described below. The transwells are assembled with an annular spacer and a polycarbonate membrane insert thus forming a disk-shaped chamber of 6 mm diameter and 50 μm height [volume ~ 2 μL] that confined the cells during the fluid perfusion of microphysiometer experiments. This cell capsule is placed in a flow and temperature (37 °C) regulated sensing chamber of the microphysiometer so that the lower membrane is in diffusive contact with the surface of the LAPS chip, and pH changes were monitored at the sensor surface in an area of 2.5 mm^2 in the center of the chamber.

Cells are perfused with HEPES-buffered balanced salts solution [BSS] containing 138 mM NaCl, 5 mM KCl, 0.5 mM $MgCl_2$, 1.3 mM $CaCl_2$, 0.81 mM Na_2HPO_4, 0.11 mM NaH_2PO_4, and 1 mM HEPES, pH= 7.4, +/- study compound at the indicated concentration, in a cyclic manner automatically controlled by a peristaltic pump. The pump cycle is 150 sec. in duration, comprising a flow-on period (100 $\mu L\ min^{-1}$ for 110 sec.) followed by a flow-off period (40 sec.). Extracellular acidification rates are determined from the slope of a linear least-squares fit to the relation of sensor output voltage versus time during the central 30 seconds of each flow-off period. The LAPS is Nernstian (61 mV= ~1 pH unit at 37 °C), so a rate of change of sensor output voltage of 1 $\mu V\ sec^{-1}$ corresponds closely to an extracellular acidification rate of 1 $x10^{-3}$ pH unit min^{-1}. Acidification rate data are mathematically normalized to 100% at the data point just prior to addition of cytoprotectant (basal acidification rate). Normalization of acidification rates allows for direct comparison of rate data collected from separate chambers with different initial rates and takes into account the variation in the number of cells deposited above the active sensing region of the LAPS chip.

IV. Results

IV.A. WIF-B Cells

WIF-B cells, a liver derived cell line, were perfused in the microphysiometer systems as described in the Methodology section. ATP depletion was effect by inclusion of the mitochondrial uncoupler, 2-4, dinitrophenol [DNP] [figure **1**]. Cells were perfused with DNP +/- GAL-4, an experimental compound. Following ~20 min of GAL-4 or glucose perfusion, WIF-B cells maintained 100% of there resting metabolic rate [proton flux]. Administration of DNP to the perfusate resulted in an ~50% increase in metabolic rate. Following ~1hr of DNP treatment metabolic rate decreased to ~30%. Removal of DNP from WIF-B cells that received glucose, failed to result in metabolic rate recovery. Cells that received GAL-4 experienced a marked increase in metabolic rate upon DNP removal, ~3x, followed by a recovery to a rate ~20% over basal conditions.

LDH release was assessed [data not shown]. Cells receiving glucose release >80 % of cellular LDH, while those receiving GAL-4 released ~10-15% LDH. These data are consistent with the protective effect of GAL-4 on isolated primary hepatocytes, and demonstrate the utility of examining proton flux recovery as a proxy for cell viability.

IV.B. CaCo-2 Cells

CaCo-2 cells, an intestinal derived cell line, were perfused in the microphysiometer as described in the Methodology Section [figure **2**]. ATP depletion was effected by administration of DNP. Removal of glucose from the cell perfusate resulted in a prompt ~60% reduction in metabolic rate. Replacement of glucose after 10 minutes of - glucose restored metabolic rate to baseline conditions. In contrast to WIF-B cells, DNP administration failed to elicit a marked increase in metabolic rate [cf. figures **1** & **2**]. Interestingly, those cells perfused in the absence of glucose exhibited a more marked response to DNP administration [cf. channels B & D, figure **2**]. Removal of glucose in the absence of DNP, resulted in a reduction in metabolic rate to ~10%. Interestingly, the absence of substrate [glucose] was not associated with untoward effects, ie., metabolic rate recovered to ~95% of baseline values. Similarly, cells perfused in the presence of DNP (-)glucose recovered ~95% of baseline metabolic rate. These data are consistent with the highly glycolytic nature of the CaCo-2 cells, i.e., a minimal dependence on oxidative phosphporylation for maintence of cell energy demands.

IV.C. MDCK Cells

MDCK cells, a renal tubule derived cell line, were perfused in the microphysiometer as described in the Methodology Section [figure **3**]. ATP depletion was effected by perfusing cells with DNP and the electron transport inhibitor antimycin A [a mixture of antimycin $A_{1\&3}$]. MDCK cells demonstarted a market decrease in metabolic rate in the absence of glucose, with a recovery on reintroduction of glucose into the perfusion media. Administration of DNP effected a marked plateau increase in metabolic rate, ~65%, that was reversed to a near baseline value of 75% upon removal of DNP. Cells receiving antimycin, demonstrated a transient increase in metabolic rate, however, metabolic rate recovered to a baseline value of ~100%.

The following conclusions are made: 1) MDCK cells readily metabolize glucose as evidenced by a marked decrease in proton production upon glucose removal; 2) DNP-mediated mitochondrial uncoupling results in increased proton production, suggestive of enhanced glycolytic flux to compensate in part for the absence of mitochondrial-derived

ATP; 3) antimycin $A_{1,3}$ inhibition of electron transport is associated with a non-sustained compensatory increase in metabolic rate; and 4) prolonged antimycin $A_{1,3}$ exposure is associated with a non-compensated increase in metabolic rate, suggestive of redox control over glycolytic flux. This data illustrates the differential effect of ATP depletion in the presence [antimycin $A_{1,3}$] and absence [DNP] of cellular redox stress.

IV.D. CHO Cells

CHO cells, a tumor derived cell line, were perfused in the microphysiometer as described in the Methodology Section [figure **4**]. ATP depletion was effected by perfusing cells with DNP and the electron transport inhibitor antimycin A [a mixture of antimycin $A_{1\&3}$] CHO-K1 cells metabolize glucose in preference to pyruvate. Inhibition of mitochondrial oxidative phosphorylation with dinitrophenol [DNP] potentiates glycolysis, as evidenced by an increase in metabolic rate of ~50%. The effect of both brief and long term exposure of CHO-K1 cells to DNP is reversible. Inhibition of electron transport with Antimycin $A_{1,3}$, decreased metabolic rate an additional ~15% . This effect was irreversible.

The following conclusions are made: 1) CHO-K1 cells can sustain significant function by glycolysis alone. The inhibition of oxidative phosphorylation in the presence of a glycolytic substrate such as glucose affords cellular protection to mitochondrial uncoupling; 2) CHO-K1 cells can sustain function, albeit at a reduced metabolic rate, in the absence of glycolysis, however, the inhibition of oxidative phosphorylation in this setting results in irreversible injury.

VI. Figures & Legends

VI.A. Legend to Figure 1, WIF-B Cells

Experiments were conducted as described in the text and Methodology Section. Metabolic rate is expressed as percent, relative to the rate determined at basal conditions. WIF-B cells were perfused with BSS +/- GAL-4. DNP was administered as indicated at the bottom of figure **1**.

VI.B. Legend to Figure 2, CaCo-2 Cells

Experiments were conducted as described in the text and Methodology Section. Metabolic rate is expressed as percent, relative to the rate determined at basal conditions. CaCo-2 cells were perfused with BSS +/- glucose. DNP was administered as indicated at the bottom of figure **2**.

VI.C. Legend to Figure 3, MDCK Cells

Experiments were conducted as described in the text and Methodology Section. Metabolic rate is expressed as percent, relative to the rate determined at basal conditions. MDCK cells were perfused with BSS +/- glucose. DNP and antimycin $A_{1,3}$ were administered as indicated at the bottom of figure **3**.

VI.D. Legend to Figure 4, CHO Cells

Experiments were conducted as described in the text and Methodology Section. Metabolic rate is expressed as percent, relative to the rate determined at basal conditions. CHO-K1 cells were perfused with BSS +/- glucose, pyruvate. DNP and antimycin $A_{1,3}$ were administered as indicated at the bottom of figure **4**.

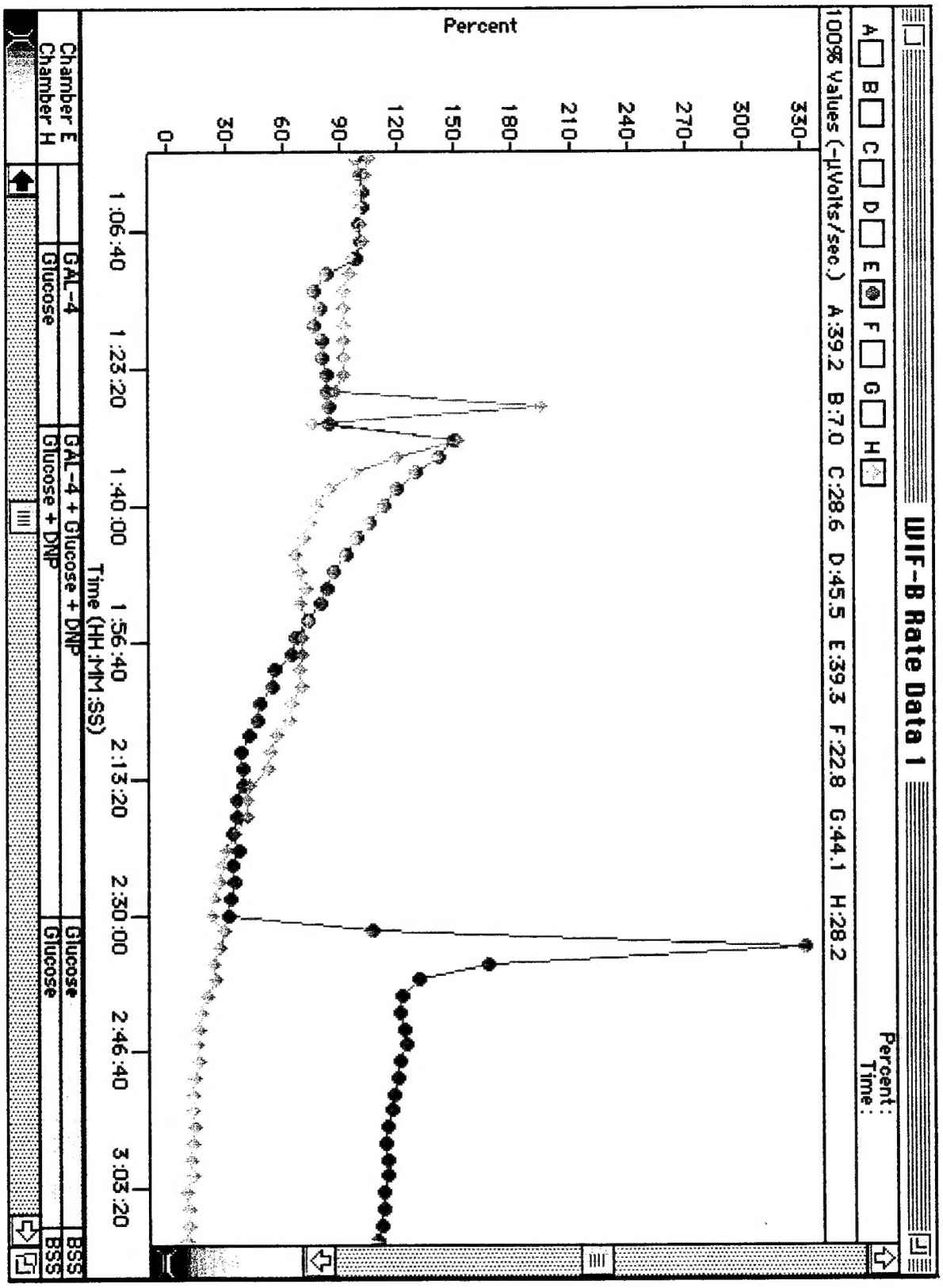
WIF-B Rate Data 1
A B C D E F G H
Percent:
Time:
100% Values (-µVolts/sec.) A:39.2 B:7.0 C:28.6 D:45.5 E:39.3 F:22.8 G:44.1 H:28.2
Percent
330
300
270
240
210
180
150
120
90
60
30
0
1:06:40
1:23:20
1:40:00
1:56:40
2:13:20
2:30:00
2:46:40
3:03:20
Time (HH:MM:SS)
Chamber E
Chamber H
GAL-4
Glucose
GAL-4 + Glucose + DNP
Glucose + DNP
Glucose
Glucose
BSS
BSS

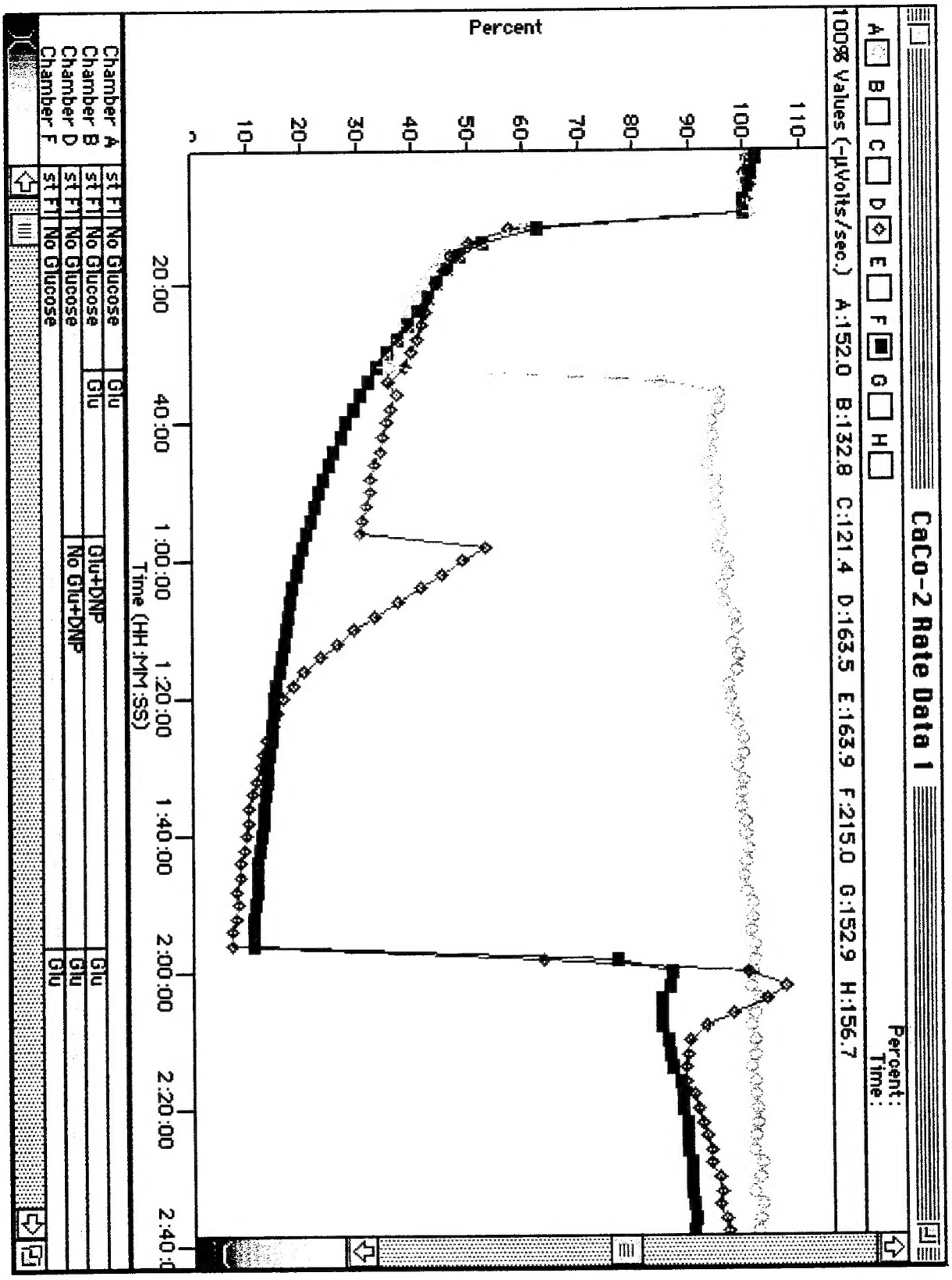
CaCo-2 Rate Data 1
Percent:
Time:
A B C D E F G H
100% Values (-µVolts/sec.) A:152.0 B:132.8 C:121.4 D:163.5 E:163.9 F:215.0 G:152.9 H:156.7
Percent
Time (HH:MM:SS)
Chamber A st F1 No Glucose Glu
Chamber B st F1 No Glucose Glu Glu+DNP Glu
Chamber D st F1 No Glucose No Glu+DNP Glu
Chamber F st F1 No Glucose Glu

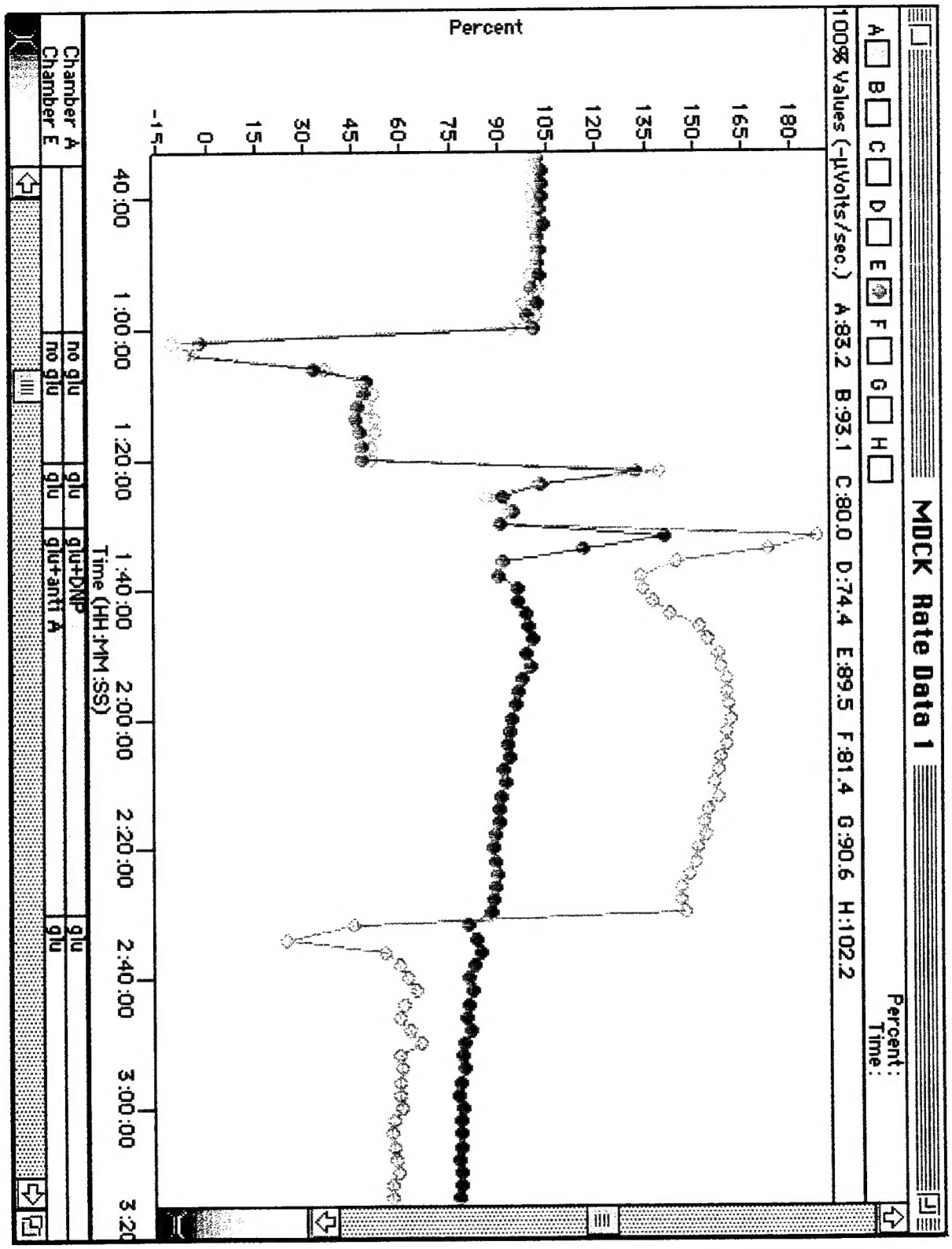
MDCK Rate Data 1
A B C D E F G H
Percent:
Time:
100% Values (-µVolts/sec.) A:83.2 B:93.1 C:80.0 D:74.4 E:89.5 F:81.4 G:90.6 H:102.2
Percent
180
165
150
135
120
105
90
75
60
45
30
15
0
-15
40:00
1:00:00
1:20:00
1:40:00
2:00:00
2:20:00
2:40:00
3:00:00
Time (HH:MM:SS)
Chamber A
Chamber E
no glu
glu
glu+DNP
glu+anti A

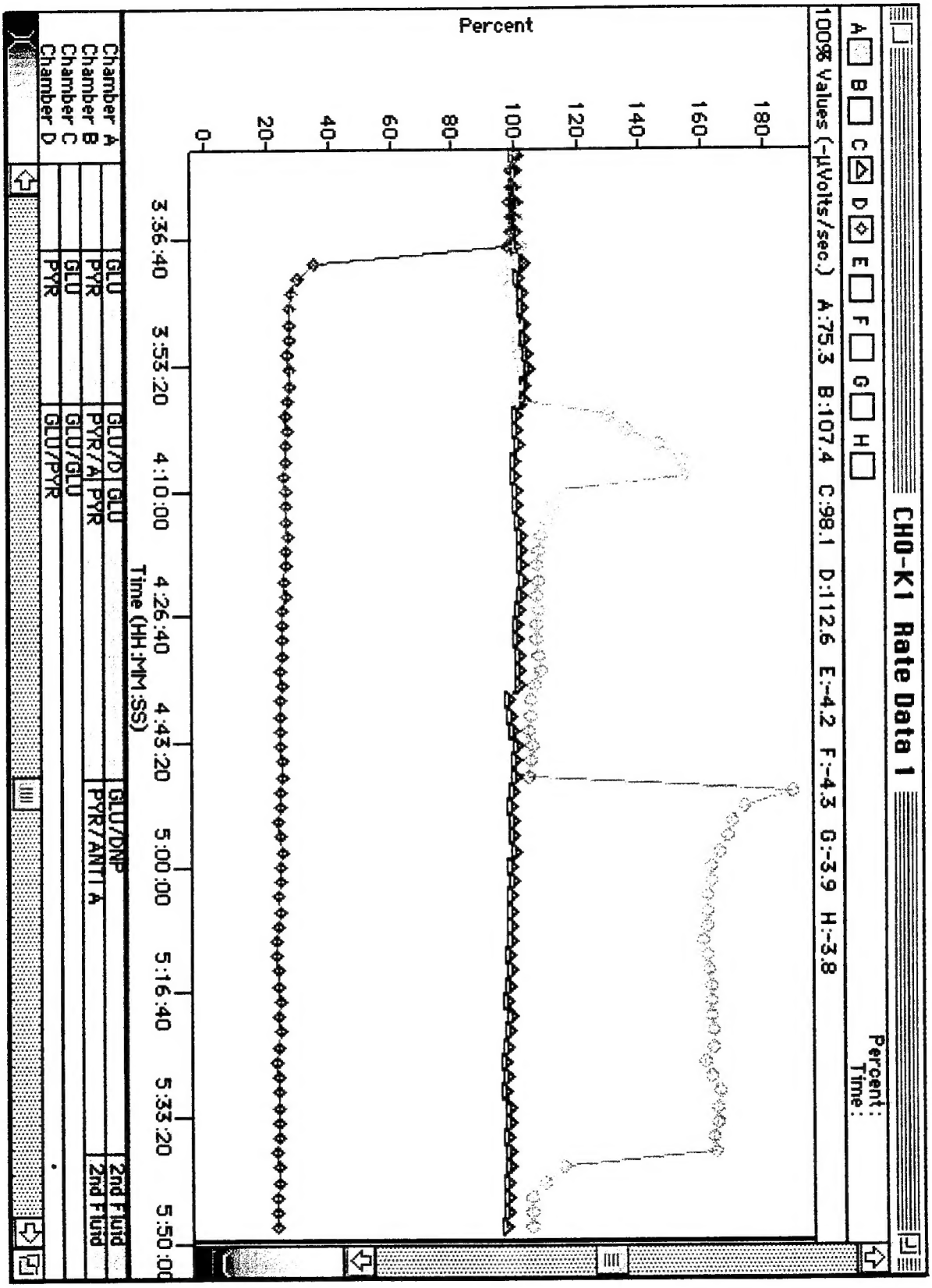
CHO-K1 Rate Data 1
A B C D E F G H
100% Values (-µVolts/sec.) A:75.3 B:107.4 C:98.1 D:112.6 E:-4.2 F:-4.3 G:-3.9 H:-3.8
Percent:
Time:
Percent
180
160
140
120
100
80
60
40
20
0
3:36:40
3:53:20
4:10:00
4:26:40
4:43:20
5:00:00
5:16:40
5:33:20
5:50:00
Time (HH:MM:SS)
Chamber A GLU GLU/D GLU GLU/DNP 2nd Fluid
Chamber B PYR PYR/A PYR PYR/ANT A 2nd Fluid
Chamber C GLU GLU/GLU
Chamber D PYR GLU/PYR